Eur Radiol (2011) 21:1077–1087
DOI 10.1007/s00330-010-2006-1

NUCLEAR MEDICINE

Usefulness of FDG PET/CT in determining benign from malignant endobronchial obstruction

Arthur Cho · Jin Hur · Won Jun Kang · Ho Jin Cho · Jae-hoon Lee · Mijin Yun · Jong Doo Lee

Received: 14 July 2010 / Revised: 17 September 2010 / Accepted: 10 October 2010 / Published online: 27 November 2010

Abstract
Objective To evaluate the usefulness of FDG PET/CT to differentiate malignant endobronchial lesions with distal atelectasis from benign bronchial stenosis.
Methods This retrospective study reviewed 84 patients who underwent contrast-enhanced chest CT and then PET/CT and had histological (n=81) or follow-up imaging (n=3) confirmation. Two chest radiologists reviewed initial chest CT and determined endobronchial lesions to be malignant or benign. Two nuclear medicine physicians reviewed PET/CT for FDG uptake at the obstruction site and measured SUV. Malignancy was considered when increased FDG uptake was seen in the obstruction site, regardless of FDG within the atelectatic lung.
Results The sensitivity, specificity and accuracy of chest CT was 95%, 48% and 84%, compared with 95%, 91% and 94% for PET/CT. Benign obstructive lesions showed statistically lower FDG uptake than malignant obstructions (benign SUV 2.5±0.84; malignant SUV 11.8±5.95, p<0.001). ROC analysis showed an SUV cut-off value of 3.4 with highest sensitivity of 94% and specificity of 91%.
Conclusion Increased FDG PET/CT uptake at the obstruction site indicates a high probability of malignancy, while benign lesions show low FDG uptake. Careful evaluation of FDG uptake pattern at the obstruction site is helpful in the differentiation between benign and malignant endobronchial lesions.

Keywords FDG · PET/CT · Lung neoplasm · Airway obstruction · Pulmonary atelectasis

A. Cho · W. J. Kang · H. J. Cho · J.-h. Lee · M. Yun · J. D. Lee (✉)
Division of Nuclear Medicine, Department of Radiology,
Yonsei University Health System,
134 Shinchon-dong, Seodaemoon-ku,
Seoul, South Korea 120-752
e-mail: jdlee@yuhs.ac

J. Hur
Department of Radiology, Yonsei University Health System,
Seoul, South Korea

Introduction

Endobronchial lesions causing distal lung collapse are routinely evaluated with high-resolution CT (HRCT) and fibre optic bronchoscopy (FOB) to rule out the possibility of malignancy. Although most endobronchial obstructive lesions are of malignant origin, differential diagnosis such as inflammation, aspiration, mucous plugs and extrinsic compression from an adjacent lymph node [1] should be considered. These endobronchial lesions are often associated with resorption atelectasis with combined pneumonia [2], which can further impede the evaluation of obstructive lesions on HRCT. Although HRCT has a high sensitivity in detecting these endobronchial lesions, it has lower specificity in differentiating benign from malignant obstructive lesions [3–6], especially in cases where the obstructing endobronchial lesions are small, and where the differentiation from common benign obstructions such as stricture or mucoid impaction might be difficult.

These endobronchial lesions with atelectasis are frequently seen on 2-deoxy-2-(F-18) D-glucose (FDG) PET/CT. As most endobronchial malignancies have concomitant chronic obstructive pneumonitis within the distal collapsed lung [1], diffusely increased FDG uptake within the collapsed lung is often seen. Subsequently, FDG uptake within malignant lesions can be obscured by the increased uptake within the distal collapsed lung in this setting.

However, regardless of the uptake within the collapsed lung, focused evaluation of the FDG uptake at the obstruction site should help in the differential diagnosis of malignant endobronchial lesions. Most benign endobronchial lesions or stricture sites should show low FDG uptake due to low cellularity or fibrosis, and malignant endobronchial lesions should show increased FDG uptake. Although fibre optic bronchoscopy and histological confirmation are the gold standard for diagnosis of these bronchial obstructive lesions, careful evaluation of FDG uptake at the obstruction site may help in characterising these endobronchial lesions before proceeding to invasive procedures. The purpose of this study was to evaluate the usefulness of FDG PET/CT to differentiate malignant endobronchial lesions with distal atelectasis from benign bronchial stenosis.

Materials and methods

Patients

The charts of 384 patients from 2005 to 2009 who presented with an endobronchial obstructive lesion with distal lung collapse were reviewed. Of those, 84 patients (66 men and 18 women, mean age 63.3 years) underwent contrast-enhanced chest CT or HRCT and then PET/CT within 30 days and had histological (n=81) or follow-up imaging (n=3) confirmation. All patients (66 male, 18 female, mean age 63.3 years, age range 29–85 years) had initial conventional chest CT or HRCT and then underwent PET/CT to further characterise the obstructive lesion or for lung cancer staging. There were generally two clinical categories for performing FDG PET/CT. (1) Either the lesion was considered to be malignant on chest CT and underwent tumour staging with PET/CT, or (2) the lesion was considered to be malignant on chest CT, but FOB biopsy results were inconclusive or benign, and further characterization was done with PET/CT. The average interval between chest CT and PET/CT was 16 days, the mean time interval between initial chest CT and fibre optic bronchoscope (FOB) was 11 days, and the time difference between PET/CT and operation was 9.7 days. Final diagnosis was confirmed either by bronchoscopic biopsy (n=44) or surgical resection (n=37), or followed up with HRCT or PET/CT for at least 1 year (n=3). Demographic data of the patients are shown in Table 1. The protocol for this study was approved by the Institutional Review Board at our institution.

Table 1 Patient characteristics

Characteristics	Value
Total patients (n)	**84**
Gender (Male : Female)	66 : 18
Mean age±SD (y)	63.3±10.5
Age range (y)	29–85
Collapse	
Segmental (n) (malignant : benign)	39 (31 : 8)
Lobar (n) (malignant : benign)	45 (37 : 8)
Histopathology	
Malignant (n) (male : female)	63 (53 : 10)
Benign (n) (male : female)	18 (11 : 7)
Confirmation method	
Fibre optic bronchoscope (n)	**44**
Malignant obstruction (n)	31
Benign obstruction (n)	13
Fibre optic bronchoscope and surgical resection (n)	**37**
Malignant obstruction (n)	32
Benign obstruction (n)	5
Imaging follow-up (n)	**3**

CT protocol

Computed tomography was performed with a 16-channel MDCT (Somatom Sensation 16, Siemens, Forchheim, Germany) or a 64-channel MDCT (Sensation 64, Siemens). Imaging was performed using the helical technique during a single breath-hold after the injection of contrast material with the patients in the supine position. A total of 100–130 ml of iopromide (Ultravist 300; Schering, Berlin, Germany) was administered intravenously at a rate of 3–4 ml/s in all patients using a power injector (Envision CT; Medrad, Pittsburgh, PA, USA). Imaging acquisition was initiated immediately after reaching enhancement of the thoracic aorta up to 100 Hounsfield Units (HU) as measured using a bolus-tracking technique. To obtain CT images, we used the following parameters: 120 kVp, 130 effective mAs, 0.5-s gantry rotation, 0.75-mm collimation and a 0.5-mm interval. Two image sets were reconstructed with a thickness of 5.0 mm and 1.0 mm using a standard algorithm from the same raw data. The imaging area ranged from the lung apices to the level of the middle portion of both kidneys. All the images were analysed in the mediastinal and lung window settings. All CT images were retrieved on a picture archiving and communication system (Centricity; GE Medical Systems, Milwaukee, WI, USA) to freely handle the images for the evaluation of lesions.

PET/CT protocol

All patients underwent routine FDG PET/CT either with DSTe PET/CT (GE Healthcare) or with Biograph TruePoint 40 PET/CT (Siemens Medical Systems, CTI, Knoxville, TN, USA). All patients fasted for at least 6 h and glucose

levels in the peripheral blood in all patients were confirmed to be 140 mg/dL or less before FDG injection. Approximately 5.5 MBq/kg of body weight of FDG were administered intravenously 1 h before image acquisition. After the initial low-dose CT (DSTe: 30 mAs, 130 kVp, Biograph TruePoint: 36 mAs, 120 kVp), a standard PET imaging protocol from the neck to the proximal thighs with an acquisition time of 3 min/bed in 3-dimensional mode was taken. Images were then reconstructed using the ordered subset expectation maximisation (2 iterations, 20 subsets).

Imaging analysis

The CT images were retrospectively reviewed and analysed by two experienced radiologists independently. The readers were aware of the study protocol, but blinded to the results of the other imaging techniques and endobronchial findings. Differences in the radiologists' assessments were resolved by consensus. Criteria for malignant obstruction were as follows [5–7]: 1. An obstructing endobronchial mass that produces a convex bulging contour to the proximal portion of the collapsed pulmonary lobe or segment. 2. Abrupt bronchial cut-off from an obstructing endobronchial mass. 3. A central or perihilar mass with submucosal or circumferential infiltration of the bronchi. 4. A malignant tumour is suggested when the obstructive lesion shows a central irregular lesion of low attenuation in comparison with dense peripheral collapsed lung parenchyma. Criteria for benign obstruction were as follows [1, 8–11]: 1. Focal, smooth and thin-walled narrowing of the bronchus. 2. Stenosis or obstruction with external compression by granulomatous lymph node enlargement. 3. Typical radiological findings (smooth border, fat or calcified components) for benign endobronchial obstructive lesions such as hamartoma or lipoma. The probability of malignant or benign obstruction was graded by using a five-point scoring system (1 = no lesion, 2 = definitely benign, 3 = probably benign, 4 = probably malignant, 5 = definitely malignant). Grades 4 and 5 were both considered to be positive.

Two experienced nuclear medicine specialists who were unaware of the clinical information interpreted the PET images qualitatively by visual inspection. Visual analysis was performed on a GE AW4.0 workstation. PET/CT fusion images were first used to trace the patient bronchus until the obstruction site, and FDG uptake at the obstructive lesion was evaluated. Malignant obstruction was considered when FDG uptake was visibly increased at the obstruction site, regardless of the FDG uptake within the distal collapsed lung. FDG uptake higher than the mediastinum was considered to be malignant. Each lesion was graded according to a five-point scoring system (1 = no lesion, 2 = definitely benign, 3 = probably benign, 4 = probably malignant, 5 = definitely malignant). Grades 4 and 5 were both considered positive.

Semi-quantitative analysis was performed by drawing a region of interest (ROI) at the obstruction site and measuring the maximum standard uptake value (SUV). ROI site selection on PET/CT fusion images was done by tracing the patent bronchus of the affected lung on CT images and drawing the ROI on PET images at the level of bronchial obstruction. ROI size was variable as it was drawn only on the intraluminal portion of the obstructive lesion. In cases where a peribronchial mass compressed the bronchus or directly invaded the bronchus, visual analysis and ROI were drawn at the obstruction site only. Receiver operating characteristic (ROC) curve analysis of SUV measurements was used to determine the best cut-off threshold value for separating malignant from benign obstruction.

In general, there were three patterns of FDG uptake in our series, which are shown in Figs. 1, 2 and 3. The patient in Fig. 1 shows focal uptake in the obstruction site and in the distal collapsed lung, indicative of malignant obstruction with distal obstructive pneumonitis. Figure 2 shows a patient with diffuse uptake in the collapsed lung, but no significant FDG uptake in the obstruction site, indicative of benign obstruction with distal obstructive pneumonitis. Figure 3 shows a patient with focal uptake in the obstruction site without increased uptake in the collapsed lung, also indicative of malignant obstruction.

Statistical analysis

Histological findings or serial imaging findings were used as the gold standard of reference, initial chest CT and FDG PET/CT were classified as true positive, true negative, false positive or false negative for the detection of malignant cause of obstruction.

The diagnostic accuracy of the two techniques for malignancy was evaluated based on the 5-point scale scores. For each imaging technique, sensitivity, specificity, positive predictive value (PPV), negative predictive value (NPV) and accuracy were calculated. The differences in sensitivity, specificity and accuracy between chest CT and FDG PET/CT were assessed using McNemar's test. The difference in the areas under the ROC curves was compared among the two modalities.

For semiquantitative analysis, student's *t*-test was performed to evaluate the average SUV for benign and malignant obstructions.

Data were presented as mean±standard deviation. Statistical significance was considered at the threshold of a p value less than 0.05 for all statistical analysis. Statistic analysis was performed using SPSS 15.0 (SPSS, Inc., Chicago, IL, USA). Graphs were drawn using Sigmaplot 10.0 (Systat Software, San Jose, CA, USA).

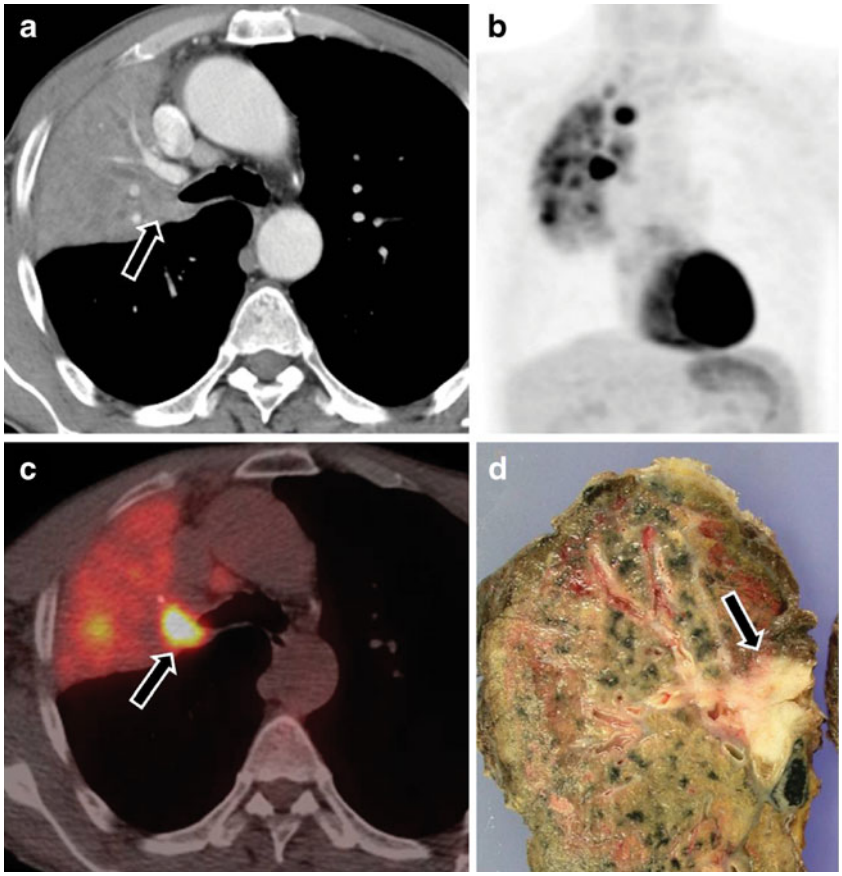

Fig. 1 Malignant obstruction with increased FDG uptake in the obstructive lesion with distal obstructive pneumonia. A 61-year-old male patient with increased FDG uptake in the entire collapsed lung with focal uptake in the obstruction site. Final pathological condition was squamous cell carcinoma. **a** Chest CT shows a right upper lung peribronchial mass with total collapse in the distal right upper lung. **b** MIP and **c** fusion PET/CT shows focal FDG uptake (SUV=13.8) in the peribronchial obstructive lesion with diffuse increased uptake in the atelectatic lung. **d** Gross histopathology images show a bronchial obstructing mass

Results

Histopathological analysis

Table 1 summarises patients' clinical profiles according to the final diagnosis. Overall, a total of 63 patients (75%) were confirmed to have malignant obstructions, and 21 patients (25%) were either histologically confirmed to have benign lesions or lesions considered benign on follow-up images.

Endobronchial obstruction was confirmed by histopathology in a total of 81 patients out of the 84 patients (96%). Of these 81 patients, 37 patients (46%) were confirmed by lobectomy or wedge resection, and 44 patients were confirmed by FOB. A total of 63 lesions were histologically confirmed to be malignant, and 18 lesions were histologically confirmed to be benign. All lesions showed bronchial obstruction or luminal narrowing on FOB. For the 18 benign lesions, 12 lesions showed total obstruction on FOB and 6 lesions showed luminal narrowing from 50% to 80%.

Three patients did not have histological confirmation, but serial chest CT or PET/CT images for at least 1 year showed that in two patients, there were no interval change in the obstructive lesion and associated atelectasis. The other one patient showed resolution of the obstruction and distal collapse without treatment in the follow-up PET/CT after 14 months, suggesting benign aetiology.

Diagnostic capability of chest CT and PET/CT

Comparison of the diagnostic capabilities of chest CT, visual analysis on PET/CT, and semiquantitative analysis on PET/CT using histopathological results as a gold standard are shown on Table 2. There was a comparable sensitivity in both chest CT and PET/CT in detecting the obstructive lesion. However, there was a statistically significant difference in specificity between initial CT and PET/CT. PET/CT showed a significantly higher specificity in differentiating benign from malignant obstructions compared with chest CT (91%, 48%, respectively, $p<0.001$), regardless of the evaluation method on PET/CT. There was no significant difference in specificity between visual analysis and SUV evaluation methods on PET/CT.

Comparison of the ROCs between chest CT and PET/CT showed that the area under the curve (AUC) was statistically higher for PET/CT than chest CT, regardless of the PET/CT evaluation method (visual PET/CT 0.93 vs 0.71, $p=0.001$; SUV PET/CT 0.96 vs 0.71, $p<0.001$). The ROC results are also shown in Table 2.

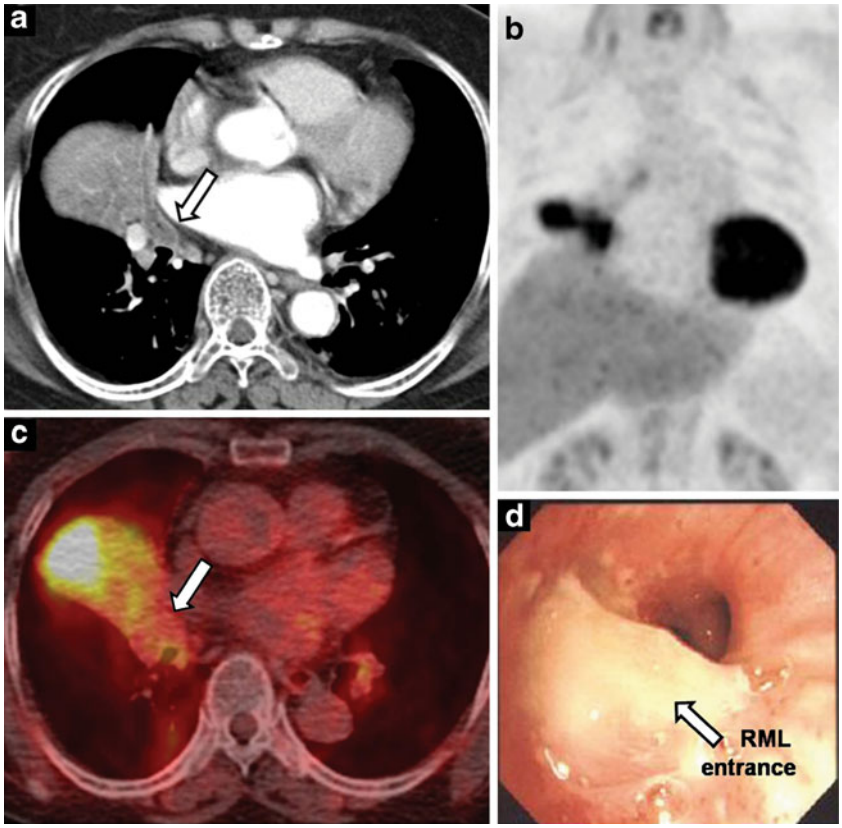

Fig. 2 Benign obstruction with no increased FDG uptake in the obstruction site with distal obstructive pneumonia. A 66-year-old female patient with increased FDG uptake in the right middle lung but no significant FDG uptake in the obstruction site. Final pathological condition was tuberculosis. **a** Chest CT shows an obstructive lesion of the right middle lobe bronchus with total collapse in the distal right middle lung. **b** MIP and **c** fusion PET/CT show no significant FDG uptake (SUV=2.9) in the obstruction site. **d** Fibre optic bronchoscopy shows a whitish exudative material obstructing the orifice of the right middle lung bronchus

Semiquantitative analysis of FDG uptake in the obstruction site showed that malignant obstruction was significantly higher (SUV 11.8±5.95) than benign obstruction (SUV 2.5±0.84, $p<0.001$, Fig. 4a). For malignant obstruction, squamous cell carcinoma and small cell lung carcinoma appeared to have higher FDG uptake (SUV 13.7±6.0, 11.5±2.5, respectively) compared with adenocarcinoma, mucoepidermoid carcinoma, carcinoid tumour, or adenoid cystic

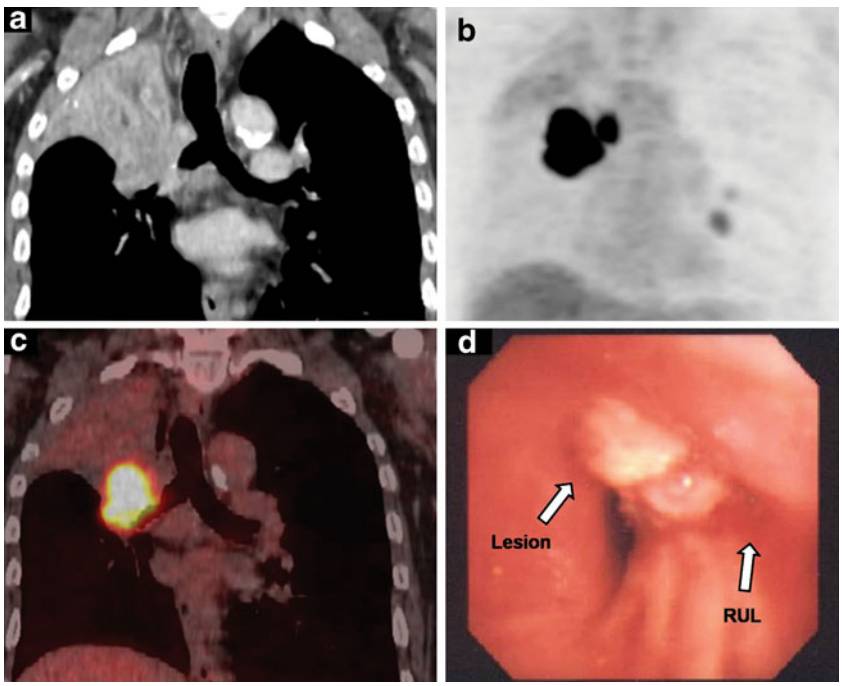

Fig. 3 Malignant obstruction with increased FDG uptake in the obstructive lesion and no uptake in the collapsed lung. A 64-year-old male patient with focal uptake in the obstruction site. Final pathological condition was squamous cell carcinoma. **a** Chest CT shows a peribronchial mass with distal atelectasis in the right upper lung. **b** MIP and **c** fusion PET/CT show focal FDG uptake (SUV=10.4) in the obstructive peribronchial lesion. **d** Fibre optic bronchoscopy shows a whitish coloured lesion totally obstructing the orifice of the right upper lung

Table 2 Comparison of diagnostic capability of chest CT, qualitative assessed PET/CT, quantitatively assessed PET/CT for differentiation of endobronchial lesions using histopathology as the standard reference.

	Initial CT*	PET/CT Visual analysis*	PET/CT SUV*
Sensitivity	95% (60/63)	95% (60/63)	94(59/63)
Specificity	48% (10/21) [a,b]	91% (19/21) [b]	95(20/21) [a]
PPV	85% (60/71)	97% (60/62)	98(59/60)
NPV	77% (10/13)	86% (19/22)	83(20/24)
Accuracy	83% (70/84)	94% (79/84)	94((79/84)
AUC	0.71(0.61–0.81)**, [a,b]	0.93(0.85–0.97)**, [b]	0.96(0.90–0.99)**, [a]

* $p<0.001$ statistical significance for chest CT, visual analysis of PET/CT, SUV PET/CT compared with histopathology.

** 95% confidence interval (CI)

[a] $p<0.001$ statistical significance for chest CT and PET/CT using a cut-off SUV of 3.4.

[b] $p<0.001$ statistical significance for chest CT and PET/CT visual analysis

carcinoma (SUV 8.7±2.4, 1.6, 4.6, 2.7, respectively). Correlation with FDG uptake and pathological features are shown in Fig 4b and Table 3.

PET/CT was also helpful in differentiating benign from malignant obstructions in patients with combined necrotizing pneumonia (Fig. 5). Contrast enhanced CT considered both cases to be malignant obstructions, but increased FDG uptake was only seen in the malignant obstruction site.

Out of the 84 cases, the two radiologists differed in opinion in five cases. Two cases out of the five were initially considered to be benign by one radiologist. Careful re-evaluation of the obstruction site according to the CT criteria for malignant obstruction resulted in determining four lesions as benign and one lesion as malignant. Final pathology showed that three lesions were correctly considered to be benign, and incorrectly considered one lesion to be benign and one lesion to be malignant.

The two false positive cases for PET/CT in our series were one case of fibroepithelial polyp (SUV 3.0) and one case of benign obstruction by reactive lymph nodes (SUV 5.1), which was misinterpreted as an endobronchial lesion. There were three false negative cases on PET which were an adenoid cystic carcinoma (SUV 2.7), a metastatic hepatocellular carcinoma (SUV 2.3, Fig. 6) and a mucoepidermoid carcinoma (SUV 1.6).

Patient management

Out of the 84 patients, CT was false positive in 11 cases, and false negative in 3 patients. PET/CT correctly assumed 10 cases out of 11 to be benign obstructions. Of those ten patients, six patients underwent FOB only and were followed-up for a range of 9 months to 28 months. Four patients underwent surgery, despite being considered to be benign on PET/CT. However, two patients had large necrotic masses (>10 cm), and had to be resected surgically, and two patients had smaller obstructive lesions (<5 cm), but the patients insisted to have the lesions surgically

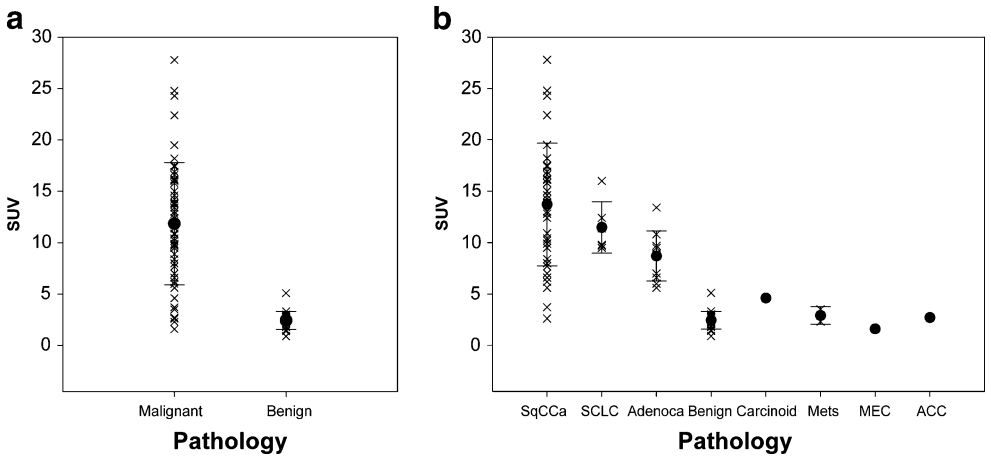

Fig. 4 Comparison of FDG uptake according to pathological condition. **a** Statistically significantly increased uptake in malignant obstructive lesions (SUV=11.96±5.93) compared with benign obstructive lesions (SUV=2.80±1.29, $p<0.001$). **b** FDG uptake according to pathological lesions.Abbreviations: Adenoca (Adenocarcinoma), ACC (adenoid cystic carcinoma), Carcinoid (Typical carcinoid tumour), MEC (Mucoepidermoid carcinoma), Mets (Metastasis), SCLC (Small cell lung cancer), SqCCa (Squamous cell carcinoma)

Table 3 Correlation of FDG uptake according to pathological condition

Pathology	Cases, n (%)	SUV±SD (range)	Statistical significance
Malignant obstruction	**63**	**11.8±5.95 (1.6–27.8)**	***P*<0.001**
Squamous cell carcinoma	42 (66.7)	13.7±6.0 (2.6–27.8)	
Adenocarcinoma	10 (15.6)	8.7±2.4 (5.6–13.4)	
Small cell lung cancer	6 (9.5)	11.5±2.5 (9.5–16)	
Mucoepidermoid carcinoma	1 (1.6)	1.6	
Adenoid cystic carcinoma	1 (1.6)	2.7	
Metastasis (HCC[a], breast cancer)	2 (3.2)	2.9 (2.3, 3.5)	
Typical carcinoid tumour	1 (1.6)	4.6	
Benign obstruction	**21**	**2.5±0.84 (0.5–5.1)**	***P*<0.001**
Chronic non-specific inflammation	10 (47.6)	2.4±0.5 (1.4–3.3)	
Chronic granulomatous inflammation	3 (14.3)	2.3±1.2 (0.9–3.0)	
Acute necrotising suppurative inflammation	1 (4.8)	2.8	
Aspergilloma	1 (4.8)	1.9	
Organising pneumonia	1 (4.8)	1.5	
Chondroid hamartoma	1 (4.8)	2.8	
Fibroepithelial polyp	1 (4.8)	3.0	
Unknown pathological condition[b]	3 (14.3)	3.2±1.7 (1.8–5.1)	

[a] *HCC* hepatocellular carcinoma

[b] Unknown pathological condition: CT or PET/CT follow-up (1–2 years) showed resolution of collapse without treatment

removed. Of the three cases considered to be benign on CT, two were correctly considered to be cancerous on PET/CT. One of these patients was re-biopsied to be confirmed to be malignant, and the other underwent surgery.

PET/CT was false positive in two cases and false negative in three cases. CT considered two of these three benign lesions to be malignant, and re-biopsy confirmed these lesions to be malignant. Of the two cases considered

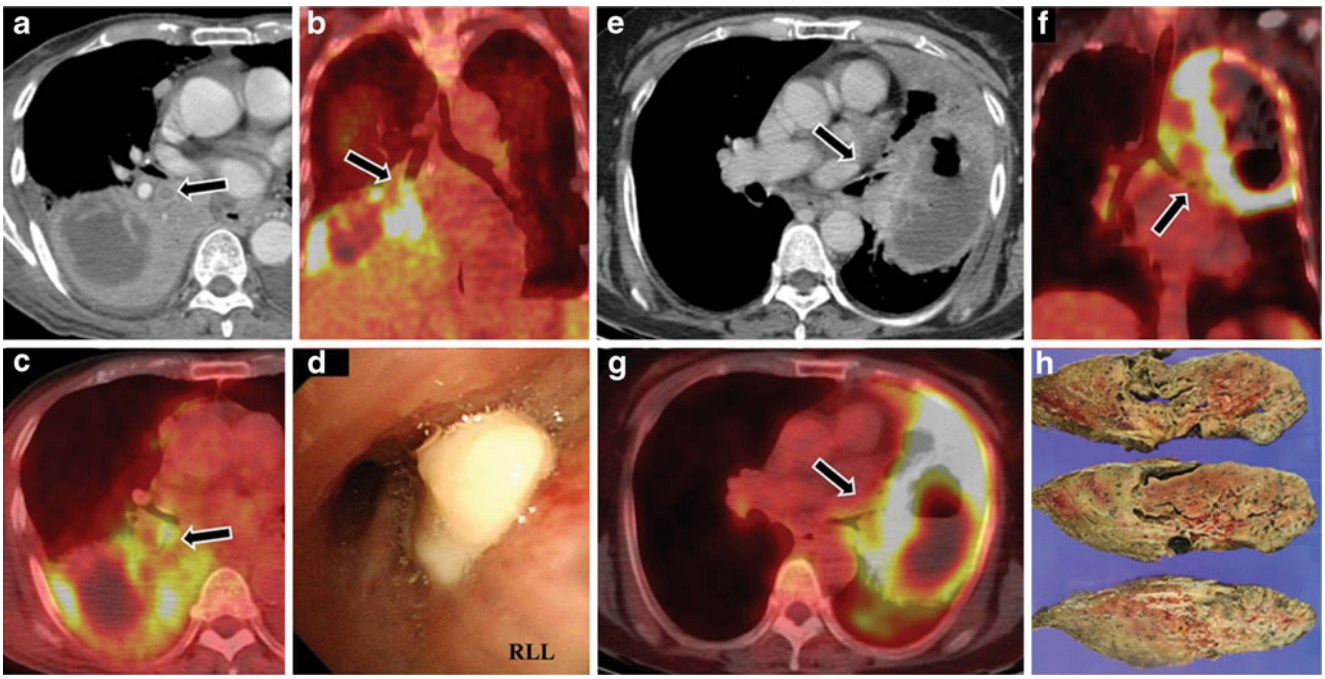

Fig. 5 Representative cases of efficacy of FDG PET/CT in differentiating malignant obstruction within obstructive necrotising pneumonia. **a**–**d** A 79-year-old male patient with a final diagnosis of squamous cell carcinoma. **a** Chest CT shows an endobronchial lesion with necrotising pneumonia within the right lower collapsed lung. **b** Fusion coronal and **c** fusion axial images show focal FDG uptake (SUV=3.7) in the obstruction site and in the distal pneumonia. **d** Fibre optic bronchoscopy shows a lesion with mass effect obstructing the right lower lung bronchial orifice. **e**–**h** A 65-year-old female patient with a final diagnosis of acute necrotising suppurative inflammation. **e** Chest CT showing obstruction in the left upper lung bronchus with obstructive necrotising pneumonia. **f** Fusion coronal and **g** fusion axial images show mild FDG uptake (SUV=2.8) at the obstruction site. **h** Gross histopathology showed an ill-defined whitish solid area with severe necrosis

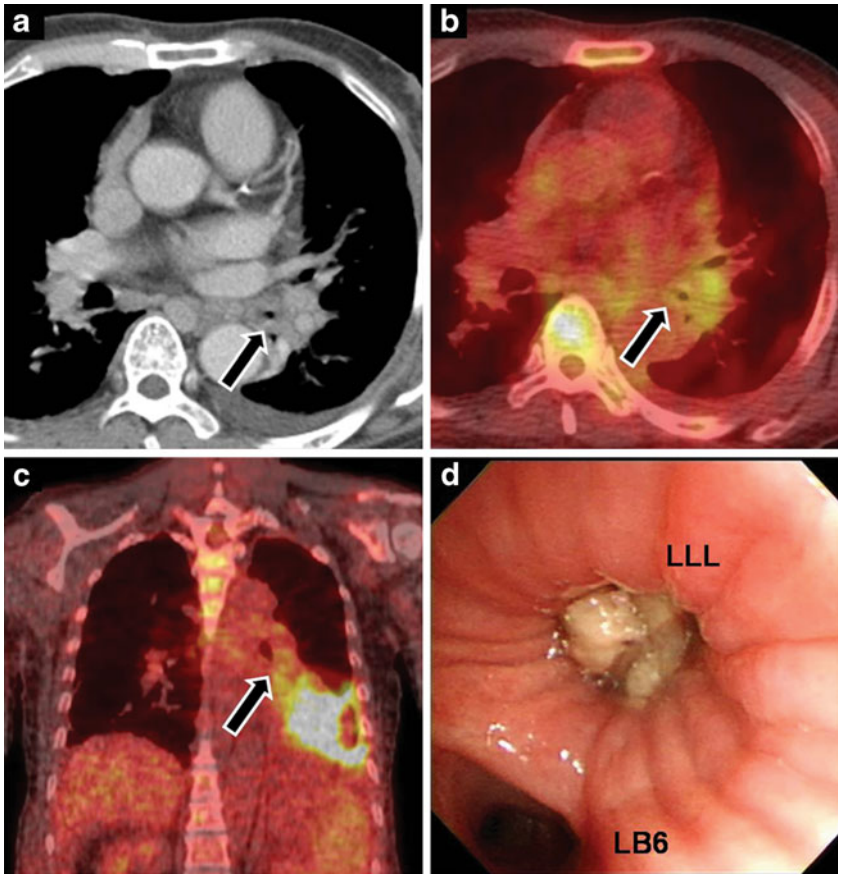

Fig. 6 A false negative case of a malignant obstructive lesion without significant FDG uptake. A 71-year-old male patient with a final pathological condition metastatic hepatocellular carcinoma. **a** Chest CT shows a peribronchial obstructive lesion of the left lower lung with lobar collapse. **b** Fusion axial and **c** fusion coronal PET/CT show no significant FDG uptake (SUV=2.3) at the obstruction site. **d** Fibre optic bronchoscopy shows a whitish endobronchial lesion obstructing the orifice of the left lower lung bronchus

to be malignant on PET, one case was considered to be benign on CT, so follow up only was done. The other lesion was also considered to be malignant on CT, so the patient underwent surgery.

Overall, PET/CT potentially reduced the number of surgeries to FOB confirmation in six patients, and confirmed malignant obstructions in two patients.

Discussion

In this study, we have shown that increased FDG PET/CT at the obstruction site indicates a high probability of malignancy, while low FDG uptake at the obstruction site is generally from benign obstructions. Therefore, careful evaluation of FDG uptake pattern at the obstruction site is helpful in characterising endobronchial lesions.

Lung atelectasis results when an extrinsic or intrinsic lesion severely obstructs the bronchus over a long period of time. Endobronchial lesions or peribronchial lesions, whether benign or malignant, will eventually compress the bronchus and cause narrowing of the bronchial lumen, which in turn, will initially lead to obstructive emphysema and then progress to atelectasis. As a result, characterisation of the obstructive lesion within the collapsed parenchyma maybe difficult as there are no definite radiological features in differentiating benign from malignant endobronchial lesions [8].

In our series, initial chest CT showed high sensitivity (95%) but significantly lower specificity (48%) in the characterisation of these endobronchial lesions. Previous reports have shown that CT has comparably high sensitivity (85–100%) [5, 12–14] in detecting endobronchial lesions, and has also shown relatively high specificity in the differentiation for benign lesions [5]. Woodring [3] reported that CT correctly identified 26 out of 26 malignant endobronchial lesions (100% sensitivity), and 20 out of 23 benign causes (87% specificity). Another report by Naidich et al. [4] demonstrated that CT correctly identified 36 of 38 malignant obstructions, and one of two benign occlusions. However, in both studies, bronchial stricture was not differentiated from malignancy in their series (false positive rates 13% and 50%, respectively). In our series, out of the 21 benign cases, 13 cases were pathologically proven to have chronic non-specific or granulomatous inflammation at the stricture site. These bronchial strictures could account for the relatively high false positive results on initial chest CT in our study.

Contrary to anatomical evaluation of these endobronchial lesions using conventional HRCT, PET combined

with CT has an advantage of evaluating the metabolism of these endobronchial lesions. Central bronchogenic tumours grow primarily within the bronchial lumen resulting in endobronchial narrowing, and peripheral neoplasms can cause bronchial obstruction either by directly invading the bronchial wall or through the centripetal flow of lymphatics [15], indicating that the obstruction site contains malignant cells. Increased FDG uptake can therefore be seen at the obstruction site for both central and peripheral lesions that cause central bronchus collapse. Conversely, benign obstructions are mostly caused by mucous plugging or post-infectious stenosis [16], which shows low FDG uptake. Rarely benign endobronchial neoplasms cause endobronchial obstruction, but these lesions are known to show minimal FDG uptake with false negativity [8, 17]. In our series, visual analysis of these endobronchial lesions with PETCT showed high sensitivity (95%) and specificity (91%). ROC analysis also showed that FDG uptake greater than 3.4 had the greatest sensitivity (94%) and specificity (91%) in differentiating malignant from benign lesions. To our knowledge, this is the first study evaluating the FDG uptake at the obstruction site within a collapsed lung parenchyma.

Previous studies with FDG PET have focused on the uptake within the collapsed lung parenchyma, to delineate the malignant foci within the collapsed lung. As we have previously stated, pneumonitis can often be seen within the collapsed lung. Chronic obstructive pneumonia, which is frequently found in endobronchial carcinomas (36% in a previous study [18]), forms when air in the obstructed lung is reabsorbed and replaced by fluid such as transudate from the capillary bed, bronchial secretions, lymphocytic infiltration of the bronchial walls, polymorphonuclear leukocytes, and parenchymal necrosis. This can then develop into the so-called golden pneumonia, which is the thickening of the interstitium by collagen and mononuclear foamy macrophages containing lipid [1, 15]. Previous studies have shown that FDG uptake within the collapsed lung itself is higher than in normal aerated lung [19], and it has been suggested that this increased FDG uptake is due to macrophages or hypoxic conditions [19–21]. Another study has shown that FDG uptake within organising pneumonia is correlated with the number of inflammatory cells [22]. Therefore, identification of malignant foci within the collapsed lung, especially in the proximal obstruction site might be difficult with FDG PET/CT as the collapsed lung can show variable uptake.

We also report two false positive and three false negative cases on PET/CT. False negative cases were adenoid cystic

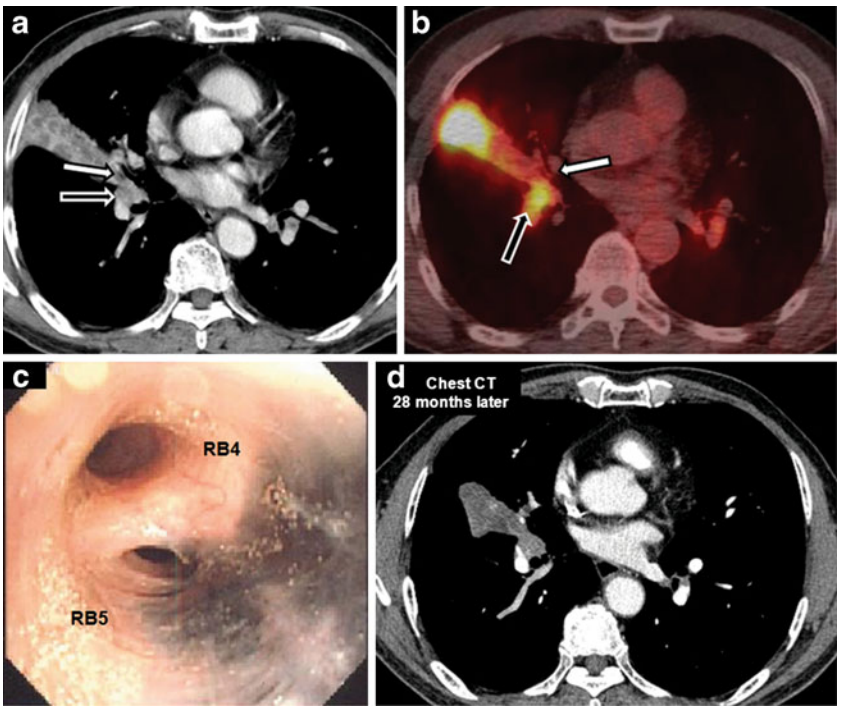

Fig. 7 A potential pitfall case of granulomatous lymph node externally compressing the bronchus. A 71-year-old male patient with collapse of the lateral segment of the right middle lung. **a** Chest CT shows right middle lobe lateral segment collapse without an obstructive lesion (*white arrow*). Note the right hilar lymph node (*black arrow*). **b** Fusion PET/CT shows no significant FDG uptake (SUV=2.7, *white arrow*) at the stricture site. The adjacent lymph nodule shows increased FDG uptake (SUV=5.4, *black arrow*). **c** Fibre optic bronchoscopy revealed multiple anthracotic pigmentation in the bilateral bronchus, and 80% luminal narrowing in the orifice of the lateral segment of the right middle bronchus with no endobronchial lesion. **d** Follow-up chest CT after 28 months shows no interval change in the collapsed lung or in the lymph node

carcinoma, mucoepidermoid carcinoma and endobronchial metastasis from hepatocellular carcinoma. These tumours are known to show low FDG uptake on PET/CT [17]. False positive cases in our series were fibroepithelial polyp and one case of enlarged LNs compressing the lobar bronchus. A potential pitfall and possible false positives that needs to be considered during the evaluation of FDG uptake in an endobronchial obstruction site are reactive lymph nodes compressing the bronchus and active endobronchial tuberculosis. As seen in Fig. 7, granulomatous mediastinal lymph nodes can extrinsically compress the bronchus and cause distal lung collapse. Initial chest CT of this patient showed right middle lung collapse and enlarged hilar lymph node, and suggested the possibility of lung cancer. FDG PET/CT showed increased uptake at the hilar lymph node, but no significant uptake at the obstruction site, suggestive of benign aetiology. FOB showed anthracotic pigmentation and stricture**,** suggestive of anthracofibrosis [23]. Follow-up chest CT 2 years later showed no interval change in the stricture and distal collapse. This case represents the importance of tracing and correlating FDG uptake at the obstruction site in differentiating malignant from benign obstruction. Another potential false positive aetiology with FDG PET/CT could be active endobronchial tuberculosis. Airway tuberculosis has been reported in 10–20% of all patients with pulmonary tuberculosis [24]. The clue in differentiating active endobronchial tuberculosis from malignant obstruction with FDG PET/CT could lie in careful tracing of the obstruction site. Active endobronchial tuberculosis usually presents with irregular airway narrowing along a long segment with wall thickening, whereas chronic or fibrotic endobronchial tuberculosis usually presents with smooth airway stricture and thin walls [10, 24–26]. Although not seen in our series, active tuberculosis would show a long segment of increased FDG uptake. Whereas in long-standing endobronchial tuberculosis the fibrotic stenosis site should show no or low FDG uptake with possible increased uptake at the adjacent granulomatous lymph node, as seen in our series.

Previous meta-analyses of the diagnostic ability of FDG PET/CT in the identification of pulmonary nodules and masses have reported high sensitivity and intermediate specificity of 0.96 and 0.78 for dedicated PET [27]. However, most of these studies have focused on solitary pulmonary nodules (SPN) or evaluated the FDG uptake of the malignant lesion itself only. Although there have been a few studies on the FDG uptake in evaluation of central airway lesions [28–33], to our knowledge, there have been no reports evaluating the FDG uptake pattern at the obstruction site in patients with endobronchial lesions with distal atelectasis.

The clinical implications for the additional benefit of PET/CT in patient management can be seen in our study, as PET/CT reduced further invasive studies in six patients and helped in confirming malignancy by determining the biopsy sites in two patients.

Our study has some limitations. There could be a case selection bias, as definite benign occlusions on CT would not be further evaluated by PET/CT, thus lowering the specificity of CT. Another potential limitation is that the final aetiology of three out of the 21 lesions was not pathologically confirmed. Because of the retrospective nature of this study, there is an inevitable time difference between the initial HRCT and PET/CT, and although there was no significant change between the two imaging techniques, this can also be a potential limitation. Prospective studies will help clarify the role of FDG PET/CT in characterising endobronchial obstructive lesions.

In summary, we have shown that increased FDG PET/CT at the obstruction site indicates a high probability of malignancy, while benign lesions show low FDG uptake. Careful evaluation of the FDG uptake pattern at the obstruction site is helpful in characterising endobronchial lesions.

References

1. Woodring JH, Reed JC (1996) Types and mechanisms of pulmonary atelectasis. J Thorac Imaging 11:92–108
2. Burke M, Fraser R (1988) Obstructive pneumonitis: a pathologic and pathogenetic reappraisal. Radiology 166:699–704
3. Woodring JH (1988) Determining the cause of pulmonary atelectasis: a comparison of plain radiography and CT. AJR Am J Roentgenol 150:757–763
4. Naidich DP, McCauley DI, Khouri NF, Leitman BS, Hulnick DH, Siegelman SS (1983) Computed tomography of lobar collapse: 1. Endobronchial obstruction. J Comput Assist Tomogr 7:745–757
5. Molina PL, Hiken JN, Glazer HS (1996) Imaging evaluation of obstructive atelectasis. J Thorac Imaging 11:176–186
6. Wilson RW, Frazier AA (1998) Pathological-radiological correlations: pathological and radiological correlation of endobronchial neoplasms: part II, malignant tumors. Ann Diagn Pathol 2:31–34
7. Naidich DP (1990) CT/MR correlation in the evaluation of tracheobronchial neoplasia. Radiol Clin North Am 28:555–571
8. Wilson RW, Kirejczyk W (1997) Pathological and radiological correlation of endobronchial neoplasms: Part I, Benign tumors. Ann Diagn Pathol 1:31–46
9. Prince JS, Duhamel DR, Levin DL, Harrell JH, Friedman PJ (2002) Nonneoplastic lesions of the tracheobronchial wall: radiologic findings with bronchoscopic correlation. Radiographics 22 Spec No: S215–30
10. Kim Y, Lee KS, Yoon JH et al (1997) Tuberculosis of the trachea and main bronchi: CT findings in 17 patients. AJR Am J Roentgenol 168:1051–1056
11. Ko JM, Jung JI, Park SH et al (2006) Benign tumors of the tracheobronchial tree: CT-pathologic correlation. AJR Am J Roentgenol 186:1304–1313
12. Henschke CI, Davis SD, Auh Y et al (1987) Detection of bronchial abnormalities: comparison of CT and bronchoscopy. J Comput Assist Tomogr 11:432–435
13. Mayr B, Ingrisch H, Haussinger K, Huber RM, Sunder-Plassmann L (1989) Tumors of the bronchi: role of evaluation with CT. Radiology 172:647–652

14. Naidich DP, Lee JJ, Garay SM, McCauley DI, Aranda CP, Boyd AD (1987) Comparison of CT and fiberoptic bronchoscopy in the evaluation of bronchial disease. AJR Am J Roentgenol 148:1–7
15. Heitzman ER, Markarian B, Raasch BN, Carsky EW, Lane EJ, Berlow ME (1982) Pathways of tumor spread through the lung: radiologic correlations with anatomy and pathology. Radiology 144:3–14
16. Grenier PA, Beigelman-Aubry C, Brillet PY (2009) Nonneoplastic tracheal and bronchial stenoses. Radiol Clin North Am 47:243–260
17. Park CM, Goo JM, Lee HJ, Kim MA, Lee CH, Kang MJ (2009) Tumors in the tracheobronchial tree: CT and FDG PET features. Radiographics 29:55–71
18. Emerson GL, Emerson MS, Sherwood CE (1959) The natural history of carcinoma of the lung. J Thorac Surg 37:291–304
19. Gerbaudo VH, Julius B (2007) Anatomo-metabolic characteristics of atelectasis in F-18 FDG-PET/CT imaging. Eur J Radiol 64:401–405
20. Kisala JM, Ayala A, Stephan RN, Chaudry IH (1993) A model of pulmonary atelectasis in rats: activation of alveolar macrophage and cytokine release. Am J Physiol 264:R610–614
21. Nestle U, Walter K, Schmidt S et al (1999) 18F-deoxyglucose positron emission tomography (FDG-PET) for the planning of radiotherapy in lung cancer: high impact in patients with atelectasis. Int J Radiat Oncol Biol Phys 44:593–597
22. Tateishi U, Hasegawa T, Seki K, Terauchi T, Moriyama N, Arai Y (2006) Disease activity and 18F-FDG uptake in organising pneumonia: semi-quantitative evaluation using computed tomography and positron emission tomography. Eur J Nucl Med Mol Imaging 33:906–912
23. Park HJ, Park SH, Im SA, Kim YK, Lee KY (2008) CT differentiation of anthracofibrosis from endobronchial tuberculosis. AJR Am J Roentgenol 191:247–251
24. Lee KS, Im JG (1995) CT in adults with tuberculosis of the chest: characteristic findings and role in management. AJR Am J Roentgenol 164:1361–1367
25. Chung HS, Lee JH (2000) Bronchoscopic assessment of the evolution of endobronchial tuberculosis. Chest 117:385–392
26. Jeong YJ, Lee KS (2008) Pulmonary tuberculosis: up-to-date imaging and management. AJR Am J Roentgenol 191:834–844
27. Ung YC, Maziak DE, Vanderveen JA et al (2007) 18Fluorodeoxyglucose positron emission tomography in the diagnosis and staging of lung cancer: a systematic review. J Natl Cancer Inst 99:1753–1767
28. Englmeier KH, Seemann MD (2008) Multimodal virtual bronchoscopy using PET/CT images. Comput Aided Surg 13:106–113
29. Erasmus JJ, McAdams HP, Patz EF Jr, Coleman RE, Ahuja V, Goodman PC (1998) Evaluation of primary pulmonary carcinoid tumors using FDG PET. AJR Am J Roentgenol 170: 1369–1373
30. Nakamura R, Ishikawa S, Sakai M, Goto Y, Minami Y (2009) Increased fluorodeoxyglucose-uptake in positron emission tomography with an endobronchial schwannoma occluding the left main stem bronchus. J Thorac Oncol 4:1183–1184
31. Pasic A, Brokx HA, Comans EF et al (2005) Detection and staging of preinvasive lesions and occult lung cancer in the central airways with 18F-fluorodeoxyglucose positron emission tomography: a pilot study. Clin Cancer Res 11:6186–6189
32. Seemann MD, Schaefer JF, Englmeier KH (2007) Virtual positron emission tomography/computed tomography-bronchoscopy: possibilities, advantages and limitations of clinical application. Eur Radiol 17:709–715
33. Tokuyasu H, Harada T, Watanabe E et al (2008) A case of endobronchial actionomycosis evaluated by FDG-PET. Nihon Kokyuki Gakkai Zasshi 46:650–654